



# Apocrine epithelial–myoepithelial carcinoma of the parotid gland with concurrent oncocytic change: a novel variant

Shu Xia, MD,<sup>a,b</sup> Xinming Chen, DDS,<sup>b</sup> Shaodong Yang, MD, DDS,<sup>b</sup> Xueqing Zheng, MD,<sup>a,b</sup> Yaying Hu, MD,<sup>a,b</sup> and Jiali Zhang, PhD, DDS<sup>a,b</sup>

Epithelial–myoepithelial carcinoma (EMCa) is a rare, low-grade, malignant salivary gland tumor. Here, we report an unusual case of an EMCa with extensive apocrine and oncocytic changes. The tumor occurred in the left parotid gland of a 68-year-old male. Histologically, the tumor was characterized by a biphasic arrangement of luminal ductal cells and abluminal polygonal myoepithelial cells, with prominent apocrine differentiation in the luminal layer and dense eosinophilic cytoplasm in both components. Immunohistochemically, the ductal epithelial component was positive for cytokeratin 7, androgen receptor, gross cystic disease fluid protein 15, and human epidermal growth factor receptor 2, and both components were diffusely positive for anti-mitochondria antibody and phosphotungstic acid–hematoxylin. EMCa with apocrine differentiation or oncocytic change is an uncommon variant. To the best of our knowledge, this report describes the first case of these 2 variants coexisting in EMCa tumor cells to be reported in the English-language literature. Awareness of the histopathologic features of EMCa is necessary to avoid making an incorrect diagnosis. (*Oral Surg Oral Med Oral Pathol Oral Radiol* 2019;128:530–537)

Epithelial–myoepithelial carcinoma (EMCa) is a rare, low-grade, malignant neoplasm, which was initially described by Donath et al. in 1972.<sup>1</sup> EMCa encompasses approximately 1% to 2% of all salivary gland neoplasms and 2% to 5% of malignant salivary gland tumors and occurs mainly in the parotid gland (60%–75%). The tumor typically occurs in the 6th and 7th decades of life and has a slight female predilection.<sup>2</sup>

EMCa is the prototypical “biphasic” salivary gland tumor that is composed of a tubular to nested bilayered arrangement of small luminal ductal cells with dense eosinophilic cytoplasm and abluminal polygonal myoepithelial cells and classically clear cytoplasm. EMCa invades in a deceptively innocuous pattern, with a multinodular pushing border. There is minimal nuclear pleomorphism and a low mitotic rate, which ranges from 1 to 4 per 10 high-power fields (HPFs).<sup>3</sup>

Although this biphasic pattern is reproduced throughout in most EMCa cases, a small subset may present a spectrum of variant phenotypes (i.e., oncocytic, spindle, clear, or sebaceous) in both cell components. These rare variants have confusing features that sometimes increase the difficulty of a differential diagnosis. For example, EMCa with oncocytic change needs to be differentiated from oncocytic carcinoma.

EMCa with apocrine differentiation may be confused with intraductal carcinoma (IDC). Double-clear EMCa gives the tumor an appearance of clear cell carcinoma. EMCa with high-grade transformation should be distinguished from another high-grade carcinoma type. To avoid misdiagnosis, EMCa with rare phenotypes need to be fully characterized histologically. This report presents a case of EMCa with apocrine and oncocytic changes in the luminal ductal cells and oncocytic changes in the abluminal myoepithelial cells.

## CASE PRESENTATION

The case was retrieved from the records of the Department of Pathology at the Hospital of Stomatology, Wuhan University (Wuhan, China). Clinical characteristics and follow-up data for the patient were obtained from the patient’s medical records. This study was conducted with approval from the local ethics committee, and consent was obtained from the patient.

A 68-year-old man presented with a painless mass of 3 months’ duration in the left parotid gland, but without obvious enlargement. The patient’s past medical history included hypertension and schistosomiasis. Palpation during the clinical examination revealed a 2.5-cm mass, which was described as firm and well-defined at the lower margin of the left earlobe. No facial palsy was noted, and no palpable lymph nodes were present in the head and neck region. The patient did not undergo preoperative magnetic resonance imaging or computed tomography examination. After the surgery, the medical advice for him was to be under observation in regular follow-up visits every 3 to 6 months. Radiation therapy or other further treatment was unnecessary unless local recurrence and metastasis occurred. However, it was found that the patient chose

<sup>a</sup>The State Key Laboratory Breeding Base of Basic Science of Stomatology & Key Laboratory of Oral Biomedicine Ministry of Education, School & Hospital of Stomatology, Wuhan University, Wuhan, China.

<sup>b</sup>Oral Histopathology Department, School and Hospital of Stomatology, Wuhan University, Wuhan, China.

Received for publication Dec 6, 2018; returned for revision Mar 4, 2019; accepted for publication Mar 25, 2019.

© 2019 Elsevier Inc. All rights reserved.

2212-4403/\$-see front matter

<https://doi.org/10.1016/j.oooo.2019.03.015>

to undergo postoperative radiotherapy at another institution. The patient was alive without any relapse or metastasis at the last date of analysis (6 months after surgery).

**MATERIALS AND METHODS**

Routine hematoxylin and eosin (H&E) staining, immunohistochemistry (IHC), and fluorescence in situ hybridization (FISH) were performed, using 4- $\mu$ m-thick sections of formalin-fixed paraffin-embedded tissue.

For IHC staining, tissue sections were incubated, with antibodies directed against the following protein makers: anti-cytokeratin 7 (Maxim, Fuzhou, China), anti-androgen receptor (AR) (Maxim, Fuzhou, China), anti-human epidermal growth factor receptor-2 (HER-2) (Maxim, Fuzhou, China), anti-calponin (Maxim, Fuzhou, China), anti-smooth muscle actin (SMA) (Maxim, Fuzhou, China), anti-p63 (Maxim, Fuzhou, China),

anti-vimentin (Maxim, Fuzhou, China), anti-S100 (Maxim, Fuzhou, China), anti-SOX10 (Maxim, Fuzhou, China), anti-gross cystic disease fluid protein 15 (GCDFP-15) (Maxim, Fuzhou, China), anti-mitochondria antibody (1:200, Novus, Littleton, CO), anti-DOG-1 (Maxim, Fuzhou, China), anti-mammaglobin (Maxim, Fuzhou, China), anti-estrogen receptor (ER) (Maxim, Fuzhou, China), and anti-Ki-67 (Maxim, Fuzhou, China). Staining with periodic acid-Schiff (PAS) with diastase digestion (Baso, Zhuhai, China) and phosphotungstic acid-hematoxylin (PTAH) (Baso, Zhuhai, China) was also performed. The overall mitotic rate was expressed as the number of mitoses per 10 HPFs using a  $\times 10$  or 22 ocular and a  $\times 40$  or 0.65 objective.

To detect *HER-2* amplification, we performed FISH by using the HER-2-DNA Probe Kit (Anbiping, Guangzhou, China).

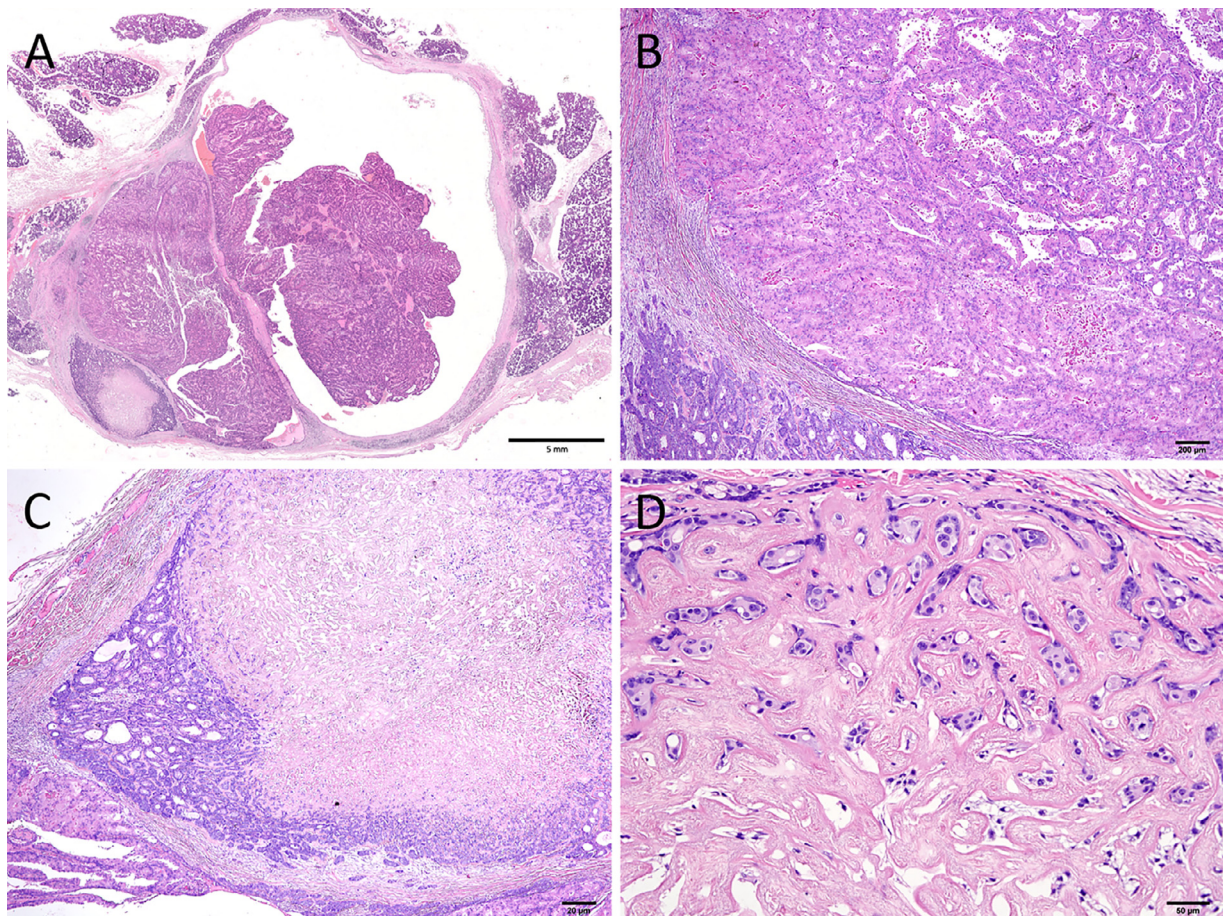


Fig. 1. (A) Low power morphology of epithelial-myoepithelial carcinoma (EMCa) with an enlarged cystic area and several solid tumor nodules (hematoxylin and eosin [H&E]; original magnification  $\times 5$ ). The tumor had a lobulated growth pattern with a well-demarcated pushing border. (B) Biphasic tubular structures with varied sizes and shapes (H&E; original magnification  $\times 40$ ). (C, D) One tumor nodule showed an area of abundant hyaline stroma at low magnification (C, H&E; original magnification  $\times 40$ ) and at high magnification (D, H&E; original magnification  $\times 200$ ). A high-resolution version of this slide for use with the Virtual Microscope is available as eSlide: [VM05571](#).

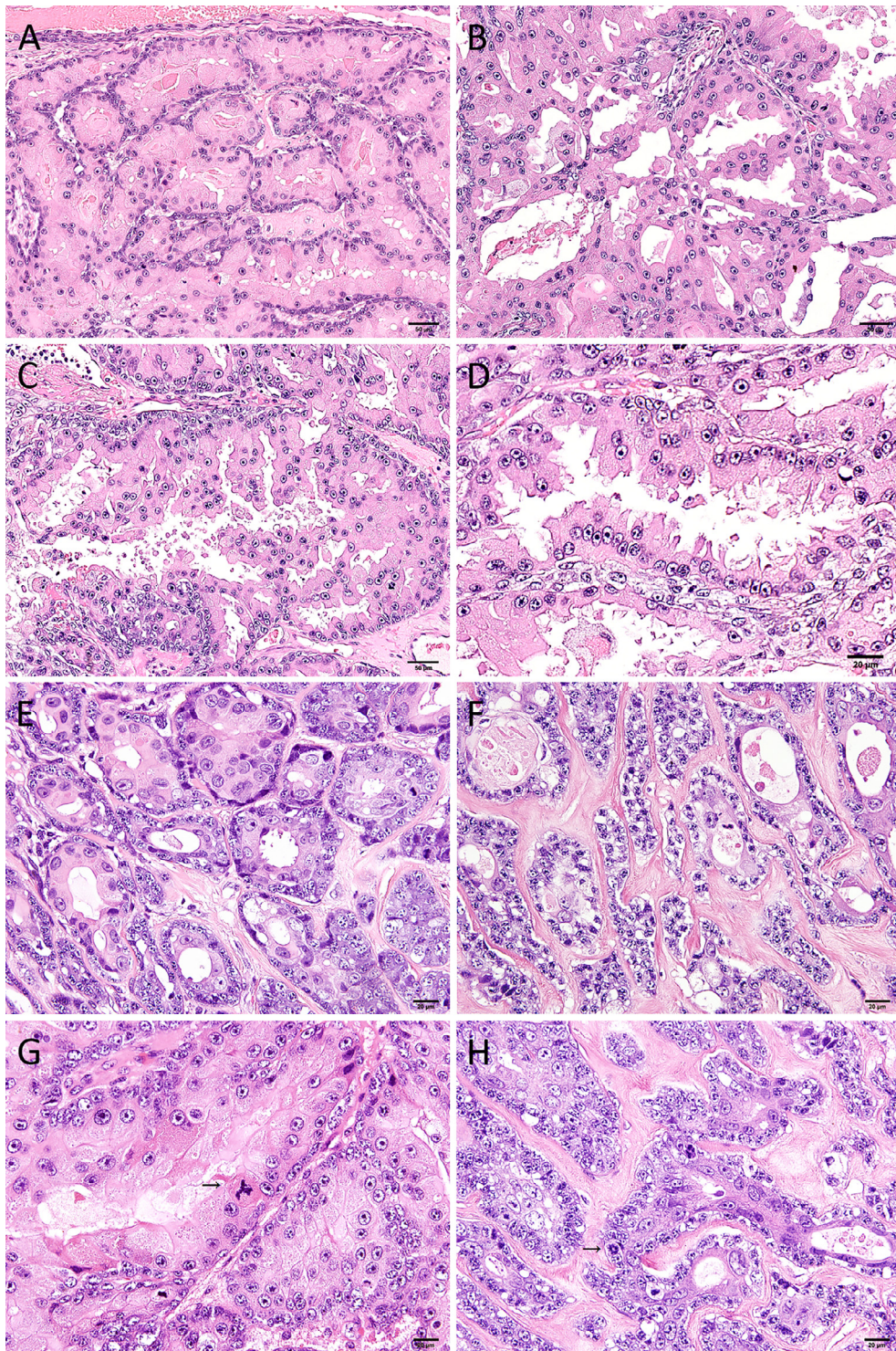


Fig. 2. (A) The tubular structure consisted of an inner layer of large, round or columnar to polyhedral ductal epithelial cells and an outer layer of polygonal myoepithelial cells (hematoxylin and eosin [H&E]; original magnification  $\times 200$ ). The cytoplasm of both cell components had abundant eosinophilic granules. (B) Cribriform pattern formed by ductal overgrowth (H&E; original magnification  $\times 200$ ). (C) The luminal ductal cells proliferated in a papillary pattern (H&E; original magnification  $\times 200$ ). (D) The ductal epithelial cells had prominent apical snouts and decapitation secretion typical of apocrine differentiation (H&E; original magnification  $\times 400$ ). (E) Hyaline stroma was observed surrounding the duct-like structures (H&E; original magnification  $\times 400$ ). (F) The myoepithelial cells with classically clear cytoplasm in the local area with the hyalinized stroma (H&E; original magnification  $\times 400$ ). (G) The arrow shows tripolar mitosis in a luminal cell (H&E; original magnification  $\times 400$ ). (H) The arrow shows ring-shaped mitosis in a myoepithelial cell (H&E; original magnification  $\times 400$ ).

**RESULTS**

**Histopathology**

The tumor was described as being 4.5 × 4 × 2 cm in size, with a circumscribed border and a solid-cystic cut surface. The tumor’s shortest axis was close to the length of the palpation diameter. There was discrepancy between the clinical size and the gross size, possibly because of the tumor location, long axis direction, and different measurement methods. Histopathologically, the tumor was surrounded by a dense stroma and exhibited a lobular configuration composed of a solid area, a cystic change area, and a hyaline stroma area (Figure 1). The tumor cells were arranged in a biphasic tubular structure, which comprised inner ductal epithelial cells and surrounding myoepithelial cells, exhibiting varied sizes and shapes (Figure 2A). The large, round or columnar to polyhedral luminal ductal cells were single-layered or proliferated in a papillary and cribriform pattern (Figures 2B and 2C). At higher magnification, the luminal cells had densely granular eosinophilic cytoplasm and round to oval vesicular nuclei, often with conspicuous nucleoli. The luminal border had prominent apical snouts and decapitation secretion, typical of apocrine differentiation (Figure 2D). The outer layer myoepithelial cells were polygonal or spindle shaped, with fine, granular, eosinophilic cytoplasm. In one area, abundant hyaline stroma was observed surrounding the duct-like structures (Figure 2E). Here, the myoepithelial cells predominated, showed overgrowth, and compressed the ductal component to such an extent that it was barely discernible. The classically clear cytoplasm of tumor myoepithelial cells could only be seen in the local area with hyaline stroma (Figure 2F).

A well-demarcated pushing border, rather than frankly infiltrative invasion, was observed in this case. Cytologically, moderate to severe cellular atypia and mitoses were frequently observed. The mean overall mitotic activity was 22 mitoses/10 HPFs. Occasionally, atypical mitoses were seen in both the luminal ductal cells and the myoepithelial cells (Figures 2G and 2H).

**IHC and histochemistry**

The immunohistochemical findings are summarized in Table I. The ductal epithelial component of the tumor was positive for cytokeratin 7, AR, GCDFP-15 and HER-2 (Figure 3). GCDFP-15-positive tumor cells comprised almost 80% of the luminal area. The myoepithelial component was positive for the calponin, SMA, P63, vimentin, SOX10, and S100 protein (Figure 4). Strong positivity for the anti-mitochondria antibody was observed in greater than 90% of both cell components (Figures 5A–5C). PTAH staining distinctly illustrated fine blue cytoplasmic granules that represented mitochondria (Figure 5D). The Ki-67 proliferation index averaged 12.8% (range 7.8%–18.1%).

**Table I.** Results of immunohistochemistry and histochemistry

Cell	CK7	AR	HER-2	GCDFP-15	Calponin	SMA	P63	Vimentin	S-100	SOX10	Mitochondria	DOG-1	Mammaglobin	ER	PAS	PTAH	Ki-67
Ductal epithelial cell	+	+	+	+	-	-	-	-	-	-	+	-	-	-	-	+	+
Myoepithelial cell	-	-	-	-	+	+	+	+	+	+	+	-	-	-	-	-	12.8%

AR, androgen receptor; CK, cytokeratin; ER, estrogen receptor; GCDFP-15, gross cystic disease fluid protein 15.

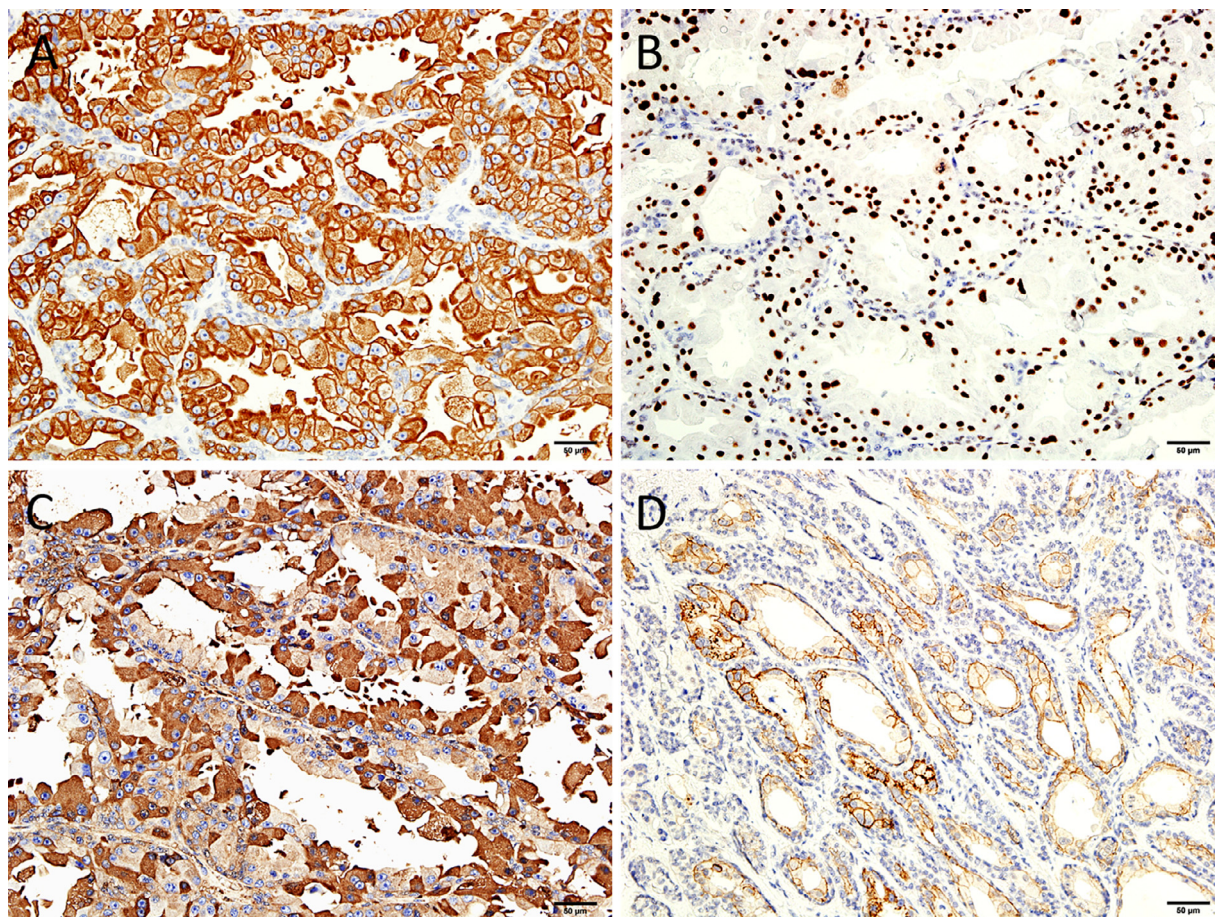


Fig. 3. (A) Cytokeratin 7 (CK7) showed strong cytoplasmic staining in the ductal component (immunohistochemistry [IHC]; original magnification  $\times 200$ ). (B) Androgen receptor (AR) showed nuclear positivity in the ductal component (IHC,  $\times 200$ ). (C) Apocrine differentiation can be highlighted by gross cystic disease fluid protein 15 (GCDFP-15) (IHC; original magnification  $\times 200$ ). (D) HER-2 staining had 2+ immunoreactivity in the membranes (IHC; original magnification  $\times 200$ ).

Other markers, such as DOG-1, mammaglobin, ER, and PAS, were negative.

#### Molecular genetic detection

FISH was performed to assess *HER-2* amplification because this case had *HER-2* IHC overexpression (2+). The *HER-2* gene was not amplified in this case.

#### DISCUSSION

EMCa is the prototypical biphasic salivary gland tumor, which is composed of a tubular to nested bilayered arrangement of the inner ductal epithelial cells and outer myoepithelial cells.<sup>2</sup> Typically, myoepithelial cells that dominate the picture in EMCa are large and polygonal and have a clear cytoplasm. The ductal component usually comprises small, lightly eosinophilic, cuboidal to low columnar cells that form tubules. Partial encapsulation and cystic change are noted in 30% of EMCa cases. Additionally, the tumor nests are often accompanied by varying degrees of hyaline sclerosis. IHC staining can be used to highlight the

biphasic appearance of EMCa. Generally, the luminal ductal components are positive for low-molecular-weight cytokeratin, whereas the myoepithelial cells are positive for p63 and muscle markers, such as SMA, calponin, and vimentin.<sup>2</sup> Similar to classic EMCa, the tumor in our case presented the characteristic biphasic tubular arrangement, focal hyaline stroma and cystic changes, and distinctive myoepithelial and ductal epithelial markers. All of these characteristics confirmed the EMCa diagnosis. However, in this case, the remarkable differences from the classic EMCa were that the tumor cells displayed oncocytic and/or apocrine changes, with variant cytologic and morphologic appearances.

Although rare, EMCa has several described variants, including EMCa with high-grade transformation, EMCa ex pleomorphic adenoma, double-clear EMCa, sebaceous EMCa, oncocytic EMCa, and apocrine EMCa.<sup>2,4-6</sup> Among them, the oncocytic and apocrine variants account for 8% of all cases.<sup>7</sup> Oncocytic EMCa was described initially by Saveria and Salama in 2005,<sup>8</sup>

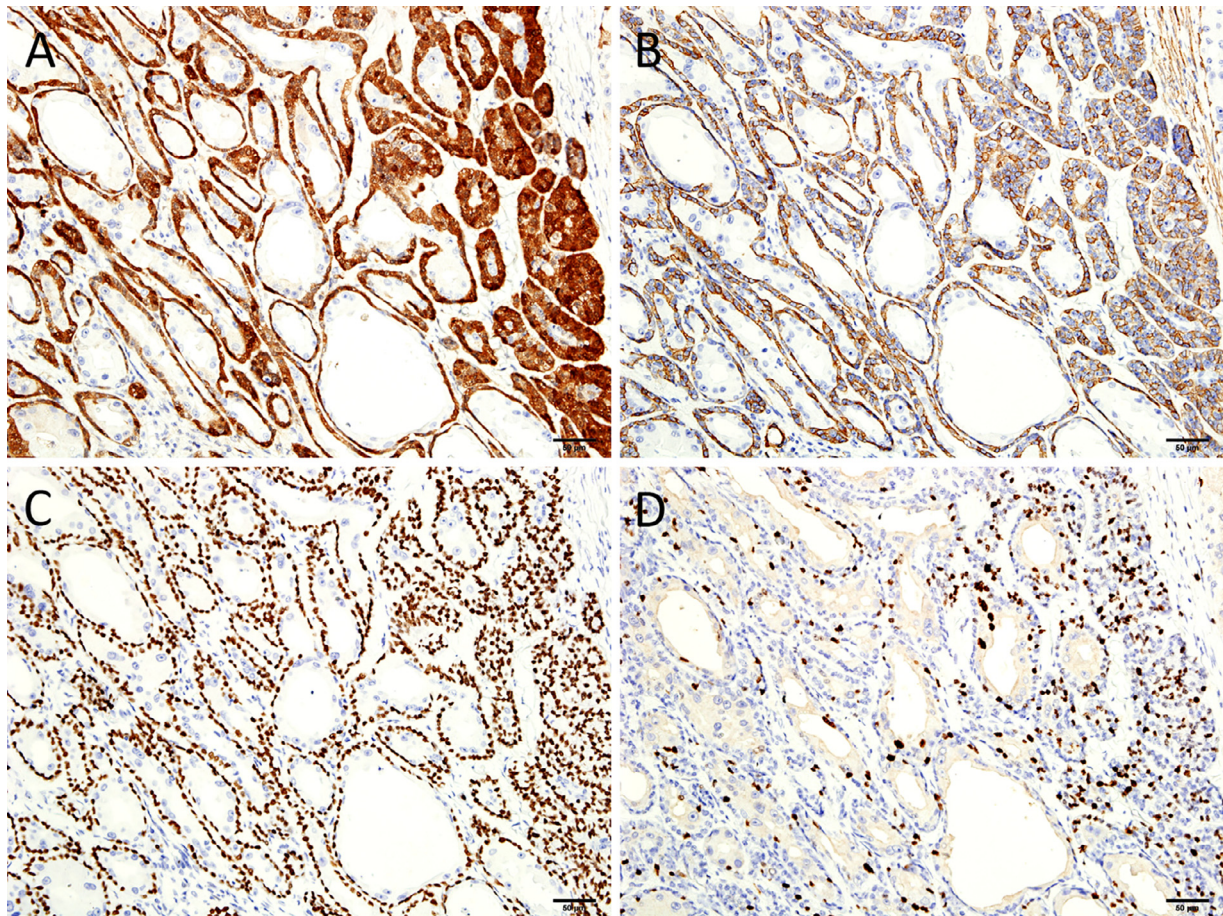


Fig. 4. (A–C) Myoepithelial cells were indicated by S100 (A, immunohistochemistry [IHC]; original magnification  $\times 200$ ), smooth muscle actin (SMA) (B, IHC; original magnification  $\times 200$ ), and P63 (C, IHC; original magnification  $\times 200$ ) IHC staining. D, The Ki-67 proliferation index was approximately 12.8%, and Ki-67 expression was seen both in the ductal epithelial cells and myoepithelial cells (IHC; original magnification  $\times 200$ ).

and apocrine EMCa was described by Seethala et al. in 2009.<sup>5</sup> Although oncocytic and apocrine changes may be seen focally in many conventional EMCa cases, generally, they are only designated as variants when the oncocytic or apocrine components comprise greater than 50% of the tumor area.<sup>7</sup>

In the case presented here, the tumor had characteristics of oncocytic and apocrine changes, moderate to high cellular atypia, and a higher mitotic index, suggesting a distinct subset of EMCa. Similar to apocrine EMCa, almost 80% of the luminal cells were large and proliferated with prominent apical snouts and decapitation secretion and were positive for AR, HER-2, and GCDFFP-15. H&E staining and the IHC results with the anti-mitochondria antibody indicated a diffuse oncocytic change in both myoepithelial cells and luminal cells. Interestingly, although this case resembled classic or apocrine EMCa because of the presence of a lobulated growth pattern, the diagnosis of “low-grade malignant tumor” should be made prudently. The evidence of cellular atypia, multipolar mitosis, a high

mitotic index (22 mitoses/10 HPFs) and the Ki-67 proliferation index in the focal area (18.1%) seemingly indicated a higher malignant phenotype. Whether this new variant has a risk of high-grade transformation or not is unknown. Long-term follow-up is necessary to assess its biologic behavior. Here, according to Seethala’s review and case reports, we summarize the main points for the identification of classic EMCa, oncocytic EMCa, apocrine EMCa, and the tumor in our case on the basis of these pathologic features, as shown in Table II.

The differential diagnosis should include salivary malignant tumors presenting with a biphasic arrangement, apocrine differentiation, and oncocytic change. The ductal structure composed of the inner ductal epithelial cells and outer myoepithelial cells was similar to that of IDC, which had been reported with prominent oncocytic change in some cases.<sup>9</sup> However, the cells surrounding the ductal component are nonneoplastic myoepithelial cells. These myoepithelial cells display small, uniform nuclei and line the basement

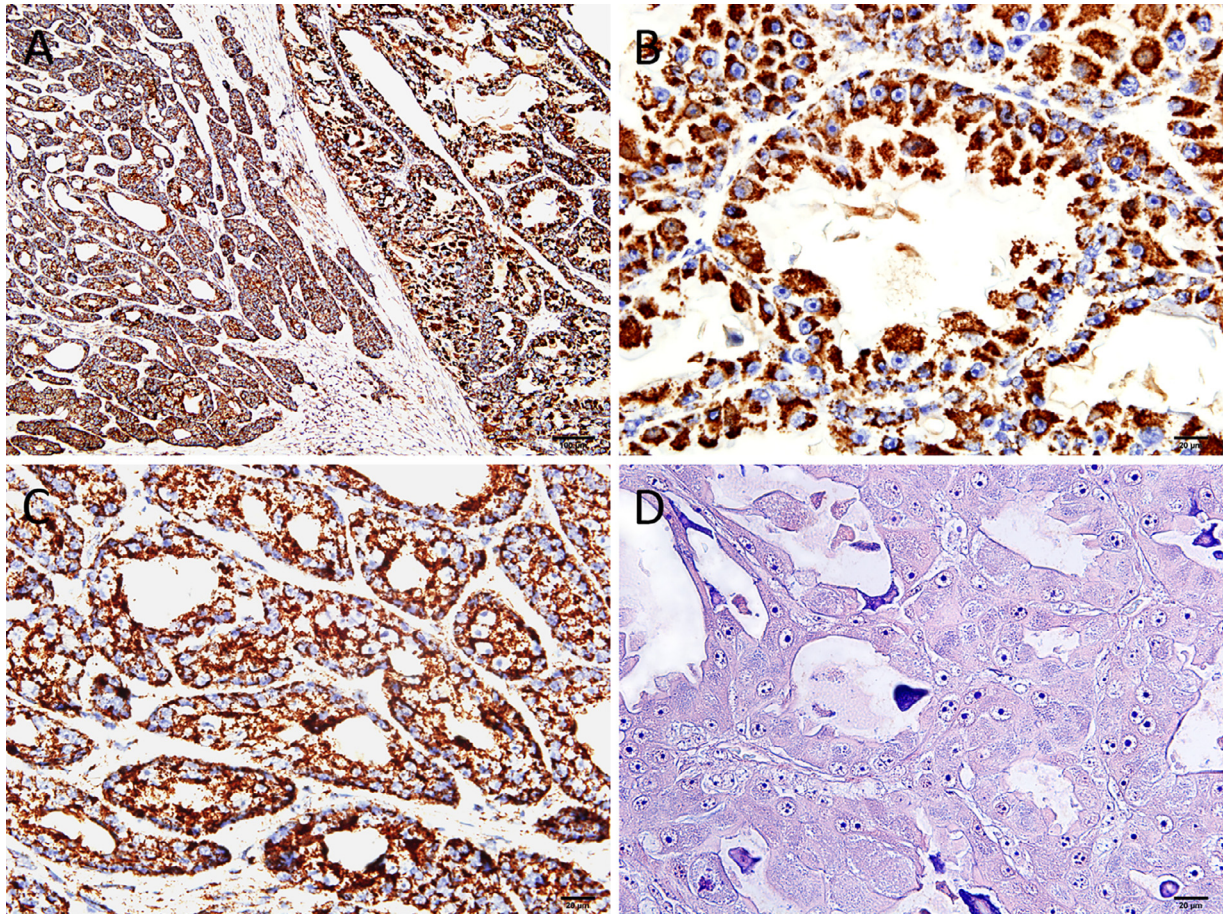


Fig. 5. (A) The oncocytic change was characterized by strong and diffuse positivity for the anti-mitochondria antibody in both the area with hyaline degeneration where myoepithelial cells predominated (left) and the cribriform region where ductal cells predominated (right) (immunohistochemistry [IHC]; original magnification  $\times 100$ ). (B) The anti-mitochondria antibody highlighted the abundant mitochondria in the ductal cells (IHC; original magnification  $\times 400$ ). (C) Myoepithelial cells (IHC; original magnification  $\times 400$ ). (D) Phosphotungstic acid–hematoxylin (PTAH) staining distinctly illustrated fine blue cytoplasmic granules (IHC; original magnification  $\times 400$ ).

membrane in an orderly manner, which is in contrast to the larger and more polygonal appearance of EMCa. Additionally, the Ki-67 proliferation index of the normal myoepithelial cells around the IDC nests is low,

whereas the tumor myoepithelial cells in EMCa show a more activated pattern. Moreover, S100 usually shows diffuse positivity in IDC, whereas it is merely expressed in the myoepithelial cells in EMCa. The

**Table II.** Pathologic differences between 4 variants of EMCa

Diagnosis	Ductal component	Myoepithelial component	Heterologous elements	Immunohistochemistry (ductal Component)	PTAH	mitoses/10 HPF
Classic EMCa	Smooth luminal surface	Clear	–	AR(–), HER-2(–), GCDFP-15(–), mitochondria(–)	–	1-4
Oncocytic EMCa	Smooth luminal surface	Clear or oncocytic	Sebaceous differentiation	AR(–), mitochondria(+)	+	
Apocrine EMCa	Apical snout and decapitation secretion	Often clear	–	AR(+), HER-2(+), GCDFP-15(+)	–	
Apocrine EMCa with oncocytic change	Apical snout and decapitation secretion	Often oncocytic	–	AR(+), HER-2(+), GCDFP-15(+), mitochondria(+)	+	22

AR, androgen receptor; EMCa, epithelial–myoepithelial carcinoma; GCDFP-15, gross cystic disease fluid protein 15.

papilocystic growth and eosinophilic cytoplasm of the tumor cells in our case raised the possibility of secretory carcinoma, which can also show apocrine morphology.<sup>10</sup> Strong and diffuse S100 protein expression and positive mammaglobin are significant for the differential diagnosis.<sup>11</sup> Furthermore, the *ETV6-NTRK3* fusion gene is specific for secretory carcinoma.<sup>12</sup> Oncocytic carcinoma is characterized by large polyhedral cells with abundant granular eosinophilic cytoplasm and round to oval vesicular nuclei arranged in solid sheets or tubular structures.<sup>13</sup> The feature of oncocytic carcinoma that is most different from that of EMCa is its negativity for muscle markers. In previous reports, oncocytic and apocrine EMCa were reported as novel variants in only 2 articles by Seethala.<sup>5,7</sup> We diagnosed the tumor in this case as apocrine EMCa with a diffuse oncocytic change on the basis of morphologic evaluation and IHC, with careful exclusion of the various differential diagnoses discussed above.

## CONCLUSIONS

This subset of EMCa has not been described previously, and this report provides for a deeper understanding of its histopathologic characteristics. Because this case is a rare variant of a rare tumor, more cases and a longer follow-up period are necessary to further elucidate its biologic behavior, prognosis, and genetic profile.

## ACKNOWLEDGMENTS

We thank Shi-chun Xiong and Yuan Li, Department of Pathology, Hospital of Stomatology Wuhan University, Wuhan, China, for their excellent technical support.

## FUNDING

This work was supported by the National Natural Science Foundation of China (Grant No. 81572664).

## REFERENCES

1. Donath K, Seifert G, Schmitz R. Diagnosis and ultrastructure of the tubular carcinoma of salivary gland ducts. Epithelial-myoeithelial carcinoma of the intercalated ducts. *Virchows Arch A Pathol Pathol Anat.* 1972;356:16-31. [in German].
2. Eveson JW, Gnepp DR, El-Naggar AK, eds. *World Health Organization Classification of Tumors: Pathology and Genetics of Head and Neck Tumors*, Lyon, France: IARC; 2005.
3. Dimitrijevic MV, Tomanovic NR, Jesic SD, Arsovic NA, Mircic AL, Krstic AM. Epithelial-myoeithelial carcinoma—review of clinicopathological and immunohistochemical features. *Arch Iran Med.* 2015;18:218-222.
4. Roy P, Bullock MJ, Perez-Ordenez B, Dardick I, Weinreb I. Epithelial-myoeithelial carcinoma with high grade transformation. *Am J Surg Pathol.* 2010;34:1258-1265.
5. Seethala RR, Richmond JA, Hoschar AP, Barnes EL. New variants of epithelial-myoeithelial carcinoma: oncocytic-sebaceous and apocrine. *Arch Pathol Lab Med.* 2009;133:950-959.
6. Shinozaki A, Nagao T, Endo H, et al. Sebaceous epithelial-myoeithelial carcinoma of the salivary gland: clinicopathologic and immunohistochemical analysis of 6 cases of a new histologic variant. *Am J Surg Pathol.* 2008;32:913-923.
7. Seethala RR. Oncocytic and apocrine epithelial myoeithelial carcinoma: novel variants of a challenging tumor. *Head Neck Pathol.* 2013;7:S77-S84.
8. Savera AT, Salama ME. Oncocytic epithelial-myoeithelial carcinoma of the salivary gland: an unrecognized morphologic variant. *Modern Pathol.* 2005;18:217a.
9. Nakaguro M, Urano M, Suzuki H, et al. Low-grade intraductal carcinoma of the salivary gland with prominent oncocytic change: a newly described variant. *Histopathology.* 2018;73:314-320.
10. Majewska H, Skalova A, Stodulski D, et al. Mammary analogue secretory carcinoma of salivary glands: a new entity associated with *ETV6* gene rearrangement. *Virchows Arch.* 2015;466:245-254.
11. Patel KR, Solomon IH, El-Mofty SK, Lewis Jr., JS, Chernock RD. Mammaglobin and S-100 immunoreactivity in salivary gland carcinomas other than mammary analogue secretory carcinoma. *Hum Pathol.* 2013;44:2501-2508.
12. Skalova A, Vanecek T, Sima R, et al. Mammary analogue secretory carcinoma of salivary glands, containing the *ETV6-NTRK3* fusion gene: a hitherto undescribed salivary gland tumor entity. *Am J Surg Pathol.* 2010;34:599-608.
13. Zhou CX, Shi DY, Ma DQ, Zhang JG, Yu GY, Gao Y. Primary oncocytic carcinoma of the salivary glands: a clinicopathologic and immunohistochemical study of 12 cases. *Oral Oncol.* 2010;46:773-778.

### Reprint requests:

Jiali Zhang,  
Associate Professor,  
Luoyu Road 237,  
Wuhan 430079,  
P.R. China.  
Jiali\_zhang@whu.edu.cn